Oxidation of model soot by NO_2 and O_2 in the presence of water vapor

R. Matarrese *, L. Castoldi, L. Lietti *

Dipartimento di Energia, Laboratory of Catalysis and Catalytic Processes and NEMAS, Centre of Excellence, Politecnico di Milano, Via La Masa, 34, 20156 Milano, Italy

GRAPHICAL ABSTRACT

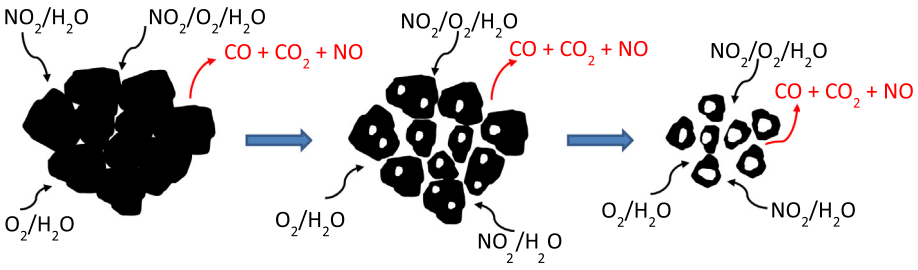

The combustion of model soot (i.e. Printex U) by NO_2 and O_2 in the presence of water was investigated in a fixed bed micro reactor under isothermal conditions. A wide range of experimental conditions (e.g. 250–350 □C, 0–5 vol% O_2, 0–500 ppmv NO_2, 0–5 vol% H_2O) were considered in order to investigate the role of NO_2, O_2 and H_2O in the combustion process. It was found that the oxidation of soot is initiated by NO_2 at temperatures where oxygen is unreactive. In addition, a synergistic effect between NO_2 and O_2 on soot combustion was observed in the presence of the NO_2-O_2 mixture. Both the direct reaction between soot and NO_2 and also the contribution of gaseous oxygen on the combustion process appeared to rise with the increasing temperature and in the presence of water. Finally, the kinetic analysis of the experimental results showed a non-negligible dependence of the kinetic parameters on carbon conver-sion and in particular the poor accuracy of the shrinking-core model at low conversion degree.

Keywords: Printex U, Diesel aftertreatment, DPF, NO_2, Soot oxidation mechanism, Oxidation kinetics

Highlights:
- Model soot (Printex U) oxidation by NO_2 and O_2 in the presence of H_2O.
- Soot oxidation initiated by NO_2 at low Temperatures.
- Synergistic effect between NO_2 and O_2 on soot combustion.
- H_2O promotion on soot oxidation.
- Dependence of the kinetic parameters on carbon conversation

1. Introduction

NO_x and particulate matter (PM or soot) emissions from both stationary and mobile diesel engines are widely recognized as an important source of pollution. In particular, diesel engines vehicles are considered as a leading source of PM emissions, which are responsible for serious human health problems, including respiratory diseases (Sydbom et al., 2001). For this reason, remarkable efforts are made by car manufacturers to explore innovative technologies to reduce polluting emissions from diesel engines, and in particular of soot. Although in the past years the development of increasingly sophisticated diesel combustion technologies has reduced pollutant emissions, nowadays the use of after-treatment technologies is mandatory to fulfil the most recent emissions standards (Twigg, 2011; Johnson and Joshi, 2017). At present, the common after-treatment technology used to reduce soot emissions consists in the employment of diesel particulate filters (DPFs) which trap the soot particles contained in the exhaust stream. In order to prevent pressure drops caused by the collection of particulate, DPFs must be periodically regenerated, generally by the temperature increase (e.g. by combustion on the filter of extra-fuel injected in the exhausts) which leads to the oxidation of the soot particles (active regeneration). More recently, the use of catalytic filters, in which DPFs are coated with a catalytic layer that favors the particulate oxidation at lower temperatures (passive regeneration), has been proposed in order to limit filter overheating and fuel consumption during the regeneration phase (van Setten et al., 2001).

Article history:
Received 27 April 2017
Received in revised form 31 July 2017
Accepted 12 August 2017
Available online 14 August 2017

* Corresponding authors.
E-mail addresses: roberto.matarrese@polimi.it (R. Matarrese), luca.lietti@polimi. it (L. Lietti).

Published Journal Article available at: http://dx.doi.org/10.1016/j.ces.2017.08.017

Aiming at the low-temperature oxidation of soot, the exploitation of NO_2 as soot oxidizing agent has been considered, being NO_2 a stronger oxidant than oxygen (Stanmore et al., 2001). This is applied in the CRT (Continuously Regenerating Trap) technology, proposed by Johnson Matthey, which consists of a pre-oxidiser which eliminates the majority of CO and unburned hydrocarbons (UHCs), followed by a filter for the particulate. The pre-oxidiser also converts NO to NO_2, which then oxidizes the particulate matter trapped in the wall-flow filter and is back-reduced to NO (Cooper and Thoss, 1989). More recently, an after-treatment system known as DPNR (Diesel Particulate-NO_x Reduction) has been developed by Toyota (Nakatani et al., 2002; Suzuki and Matsumoto, 2004). This system consists of both a catalytic filter and a specific diesel combustion technology, which has the unique capacity to remove simultaneously both soot and NO_x. The new catalytic converter for DPNR is a porous ceramic filter coated with a catalytic layer constituted by a high surface area support (e.g. γ-alumina), a noble metal and an alkaline or alkaline-earth metal oxide, which presents a high NO_x-storage capacity. These catalytic systems work under cyclic conditions, alternating a lean phase during which the NO_x produced by the engine are adsorbed on the catalyst, with a short rich phase, during which the stored NO_x are reduced to nitrogen. Under lean conditions the DPNR system works as a catalyzed soot filter in which soot oxidation occurs thanks to the presence of both NO_x and oxygen in the exhausts. In previous works from our group (Castoldi et al., 2006; Matarrese et al., 2014) the activity of model Pt-Ba/Al_2O_3 and Pt-K/Al_2O_3 catalysts in the removal of soot and NO_x according to DPNR concept have been addressed. It has been shown that under cycling conditions, i.e. alternating lean/rich phases according to the typical DPNR operation, NO_x are stored onto the catalyst surface and subsequently reduced to nitrogen. In addition, soot oxidation also occurs during the lean phase, and this has been primarily ascribed to the NO_2 formed upon NO oxidation over Pt sites. Besides, a specific role of the stored NO_x in the oxidation of soot has also been demonstrated.

In this respect many studies are available in the literature concerning the oxidation of soot by NO_x, with particular reference to NO_2 (e.g. see the very comprehensive review by Stanmore et al. (2008) and references therein) under conditions relevant to after-treatment technologies. However, a significant interest still persists on the mechanisms and kinetics of the NO_2-assisted soot combustion. In particular, despite there is a general consensus on the fact that soot oxidation with NO_2 is enhanced by the presence of O_2, different C—NO_2—O_2 reaction mechanisms have been proposed so far and the specific role of NO_2 and O_2 in the accelerated combustion of soot is still debated. Jacquot et al. (2002) attributed the large increase in the soot oxidation rate, observed when O_2 is added to the NO_2-feed gas, to the reaction between oxygen and the surface intermediates species resulting by the interaction between carbon and NO_2. Accordingly, Setiabudi et al. (2004), by correlating flow-reactor experiments with the DRIFT analysis of soot oxidation intermediates, proposed that soot oxidation is initiated by the NO_2-soot interaction that creates surface oxygen complexes which are more reactive to oxygen than pristine soot at temperatures where the oxidation with only O_2 is not significant. In agreement with this hypothesis, Müller et al. (2012) found that initially highly functionalized types of soot are less susceptible to this effect. The C—NO_2—O_2 oxidation mechanism has been also investigated by Jeguirim et al. (2004, 2005, 2007, 2009a) who suggested the occurrence of two distinct reactions: (i) a direct reaction between NO_2 and the carbon surface; (ii) a cooperative reaction involving simultaneously O_2 and NO_2. In the latter case, NO_2 has been indicated to foster the decomposition surface oxygen complexes originated by O_2. More recently, Christensen et al. (2017) ascribed the increase of soot oxidation rate, observed in the presence of NO_2, to the weaker O—NO bond in NO_2 than the O—O bond in O_2 and to the radical nature of NO_2 which are expected to favor the oxygen transfer and thus soot combustion.

Based on these considerations the aim of the present work is to further investigate the soot oxidation by NO_2 and O_2. For this purpose, isothermal combustion experiments were carried out at different temperatures and over a wide range of NO_2 and O_2 concentrations, both in the absence and in the presence of water, in order to determine the respective contribution to the combustion process in conditions close to automotive exhaust gas after-treatment.

Given that the type and structural characteristics of soot (e.g. elemental composition, surface area, particle size, degree of organization) can affect its oxidation behavior (Leistner et al., 2012; Pahalagedara et al., 2012; Sharma et al., 2012) a commercial soot (Printex U, Evonik-Degussa) was used as model soot, which is widely used as a surrogate for diesel soot laboratory experiments (Fino et al., 2016) and whose properties are well described in the literature (Atribak et al., 2010; Liu et al., 2010; Setiabudi et al., 2004).

2. Experimental

Isothermal temperature oxidation (ITO) experiments were used to evaluate the un-catalyzed soot (i.e. Printex U) oxidation characteristics. All reactivity tests were performed in a micro flow-reactor equipment consisting of a quartz tube reactor (7 mm I.D.) connected to a mass spectrometer (ThermoStar 200, Pfeiffer Vacuum) for on-line analysis of O_2, H_2O, N_2; an UV-Analyzer (Limas 11 HV, ABB) for on-line analysis of NO and NO_2 and a micro GC (Agilent 3000 A) for the on-line analysis of CO and CO_2.

The soot oxidation activity was investigated under diluted conditions in order to achieve nearly isothermal conditions thus limiting the temperature rise due to the exothermicity of the reaction. For this purpose in the tests 6 mg of soot (Printex U) were used, diluted with 100 mg of quartz powder. The reactor was inserted into an electric furnace driven by a PID temperature controller/programmer (Eurotherm 2408). The temperature of the sample was measured and controlled by a K-type thermocouple (outer diameter 0.5 mm) directly immersed in the quartz/soot bed. The total gas flow was always set at 200 cm^3/min (at 0 °C and 1 atm).

Before the isothermal oxidation tests, the soot sample was conditioned under helium at 500 °C (heating rate 15 °C/min). As suggested e.g. by Yezerets et al. (2005), this procedure removes weakly adsorbed species like adsorbed hydrocarbons (soluble organic fraction, SOF) which could affect the soot oxidation activity and hence the reproducibility of the experiments. Of note, limited mass loss was observed upon heating the soot, generally below 1–3% of the total mass. This is in line with the structure of Printex U mainly consisted of carbon framework with low fraction of volatile material (Atribak et al., 2010; Liu et al., 2010; Setiabudi et al., 2004). After this pre-treatment, the sample was cooled at the desired temperature (in the range 250–350 °C) and the reactant gas mixture for the oxidation experiment was fed to the reactor.

In the standard run the temperature was set at 300 °C and a flow of He + O_2 (5% v/v) + H_2O (2% v/v) was fed to the reactor. Then, a rectangular step feed of NO_2 (300 ppm) was admitted in the gas stream.

To investigate the influence of the individual gas components (i.e. H_2O, NO_2 and O_2) on the soot oxidation, their concentrations have been varied while keeping constant the concentration of the other components. The total gas flow rate was kept constant by adjusting the He flow.

In each test, after oxidation of up to 80% of the initial soot carbon mass, the experiment was completed upon increasing the tem-

perature at 400 or 800 °C. This led to a complete soot oxidation. The C-balance, estimated from the initial soot loading and the amounts of evolved CO_x during the whole experiment, always closed within ±5%.

3. Results and discussion

3.1. Oxidation of Printex U by NO_2-O_2 mixture

Fig. 1 shows the results obtained in the soot oxidation at 300 °C with the standard reactor feed (300 ppm NO_2, 5% O_2 and 2% H_2O in He).

Upon NO_2 admission to the reactor (t = 0 s), soot oxidation takes place and NO, CO and CO_2 evolution is observed due to the occurrence of the following global reaction:

$$NO_2 + C \rightarrow NO + CO \quad (1)$$

$$2NO_2 + C \rightarrow 2NO + CO_2 \quad (2)$$

In particular, upon NO_2 admission, an immediate formation of both CO_2 and CO is observed. CO_2 and CO concentrations initially reach a level near 60 ppm and 20 ppm respectively; then they progressively increase with time showing a maximum near 80 ppm and 30 ppm, respectively, after 11,000 s. According to literature indications, the initial increase of the oxidation rate might indicate the initial increase of the soot surface area upon combustion (Mendiara et al., 2007; Zouaoui et al., 2010). Then CO_2 and CO concentrations decrease with time on stream, due to the decrease of the soot amounts.

At 32,000 s. (i.e. at roughly 85% conversion), the NO_2 supply is switched off and a temperature programmed oxidation in O_2 and NO_2 was carried out to quantify the residual soot (not shown in Fig. 1).

Fig. 1 also shows the NO and NO_2 outlet concentrations. The sum of nitrogen oxides NO_x (=NO + NO_2) is also displayed which equals the NO_2 inlet concentration during the hole isothermal step, if one excludes the initial transient period during which the total NO_x concentration is smaller than the NO_2 inlet concentration (see inset A of Fig. 1). In particular, upon NO_2 admission to the reactor (t = 0 s), the NO outlet concentration shows a sharp maximum (ca. 300 ppm) whereas the NO_2 outlet concentration trace exhibits an initial dead time and then slowly increases. This suggests that NO_2 adsorbs onto the carbon surface in the form of nitrates ad-species, according to the stoichiometry of the following disproportionation reaction leading to the evolution of NO (Azambre et al., 2006; Shirahama et al., 2002):

$$NO_2^- + NO_2 \rightarrow NO_3^- + NO \quad (3)$$

where NO_2^- is a NO_2 adsorbed species and NO_3^- is a surface nitrate species.

After this transient regime, the NO concentration profile resembles that of CO_x, showing a maximum of 150 ppm after 11,000 s, and then decreases with time on stream. The NO_2 concentration is specular to the NO profile showing a minimum of 130 ppm after 11,000 s, and then progressively increasing near the end of the run, in correspondence of the decrease of the CO_2 and CO concentrations.

Finally, Fig. 1 also shows the values of the parameter ΔO (= $2CO_2$ + CO). This parameter accounts for the participation of gaseous oxygen in the soot oxidation. In fact, when the oxygen provided for soot oxidation comes from NO_2 alone, the ΔO trace should be superimposed to that of NO, this latter being produced according to reactions (1) and (2). If ΔO is higher than the NO concentration trace, the involvement of gaseous O_2 should be invoked to account for CO_x production. As it clearly appears from Fig. 1, the ΔO profile is higher than that of NO, indicating a substantial contribution of molecular oxygen in the soot oxidation process.

To evaluate the reactivity of soot towards O_2 only, soot oxidation experiments were also performed in the absence of NO_2 under the same experimental conditions (300 °C, 5% O_2 and 2% H_2O in He). The results are reported in the inset B of Fig. 1 in terms of CO and CO_2 production. Upon O_2 addition to the reactor (t = 0 s), negligible amounts of CO_2 are observed (near 4 ppm), without any formation of CO. This indicates that the O_2-soot reaction is

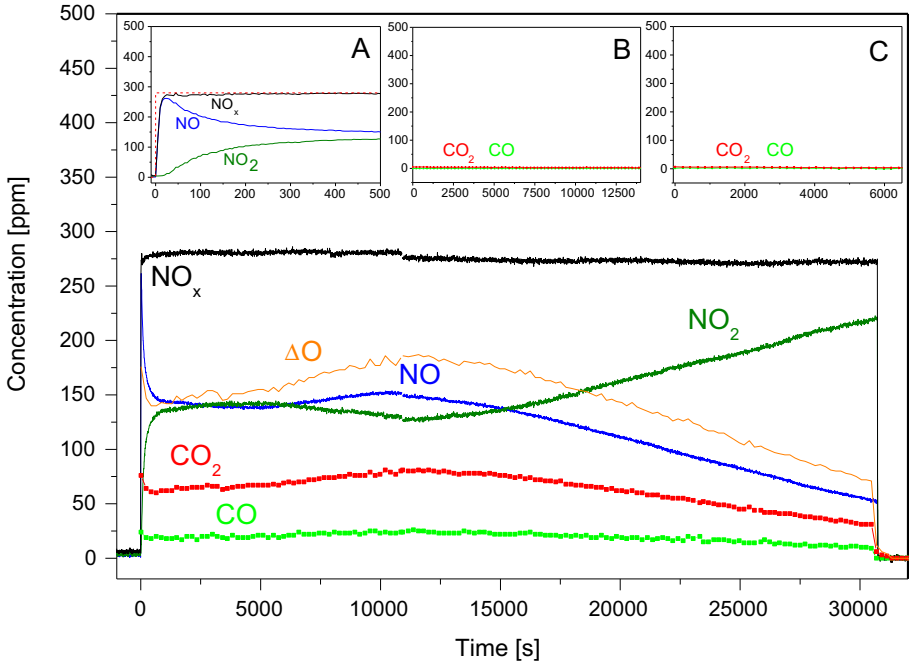

Fig. 1. Printex U oxidation at 300 °C (300 ppm NO_2, 5% O_2 and 2% H_2O). Inset A: magnification of the first 500 s. Inset B: Printex U oxidation at 300 °C in the absence of NO_2 (5% O_2 and 2% H_2O). Inset C: Printex U oxidation at 300 °C in the presence of NO and oxygen (300 ppm NO, 5% O_2 and 2% H_2O).

almost negligible in the absence of NO_2. This behavior is in agreement with the results of Jeguirim et al. (2005) who observed no significant gasification of carbon by oxygen in the temperature range 300–400 °C.

For comparison purpose, the reactivity of the NO/O_2 mixture (300 ppm NO, 5% O_2 and 2% H_2O in He) was also investigated at 300 °C. The results (see inset C in Fig. 1) show that soot oxidation is negligibly affected by the presence of NO. In fact, the evolution of both CO_2 and CO is negligible also in this case. Of note, no oxidation of NO to NO_2 (not shown in the figure) has been monitored. This result is in line with several literature reports (Jelles et al., 1999; Liu et al., 2001; Matarrese et al., 2008; Setiabudi et al., 2002), indicating that the beneficial effect of NO on soot oxidation in the presence of O_2 is observed only in the presence of a NO-oxidation catalyst (e.g. platinum), thus pointing out the key-role of NO_2 formation in the soot combustion.

To investigate more in details the oxidation of carbon by the NO_2—O_2 gas mixture and in particular to clarify the specific role of both NO_2 and O_2 a systematic study on the effect of these species was performed.

The effect of the O_2 partial pressure on the soot oxidation was investigated at 300 °C with the standard reactor feed (300 ppm NO_2, 2% H_2O in He) by varying the O_2 concentration from 0% to 10%. The results are displayed in Fig. 2A in terms of temporal evolution of m_c/m_{c0} (i.e. the residual soot carbon mass normalized by its initial value) versus time, for different O_2 contents. From Fig. 2A it clearly appears that the soot consumption rate increases upon increasing the oxygen concentration. In fact, while in the absence of oxygen the residual soot approaches 20% (e.g. 80% conversion) after ca. 70,000 s, in the presence of 1% and 5% of oxygen 80% soot conversion is attained after ca. 45,000 s and 28,000 s, respectively. Upon further increase in the oxygen concentration (up to 10%) a negligible effect on soot oxidation is observed, thus suggesting the presence of surface saturation effects in the reaction mechanism, as will be discussed at the end of this section (see below). This is also in line with the observations of Messerer et al. (2006). Fig. 2B illustrates the contribution of molecular oxygen to the soot oxidation process, pointed out by the parameter (ΔO—NO) estimated during the experiments carried out by varying the oxygen concentration in the feed. Here, ΔO accounts for the whole oxygen consumed upon soot oxidation while NO (in ppm) represents the amount of oxygen provided by the conversion of NO_2 due to reactions (1) and (2). Data are reported at different values of the soot conversion ζ. As expected, Fig. 2B shows that in the absence of molecular oxygen in the feed (O_2, 0%), the (ΔO—NO) value is, within experimental error, near to zero, because NO_2 is the only available oxidant agent. On the contrary, in the presence of oxygen (O_2, 1–10%), the ΔO value exceeds the NO concentration (i.e. the difference (ΔO—NO) is not nihil) indicating the contribution of molecular oxygen to the soot combustion. Notably, the participation of gaseous O_2 in soot combustion increases with the increasing oxygen concentration from 1% to 10% although the rate of soot oxidation is not affected at the highest concentration, as shown in Fig. 2A where it appears that the runs performed with 5% and 10% of oxygen show very similar soot oxidation rates.

Concerning the selectivity of the soot combustion towards CO and CO_2 (not shown in the figure), data show that the presence of oxygen does not significantly affect the CO_2/CO ratio which has been found close to 2.5–3.5 at all the investigated O_2 concentrations and also nearly independent of the soot conversion.

The effect of the NO_2 concentration on soot combustion was also investigated. Accordingly experiments were performed at 300 °C with the standard reactor feed (5% O_2 and 2% H_2O in He) in the presence of different NO_2 concentration, in the range 60–500 ppm. Fig. 2C shows the temporal evolution of m_c/m_{c0} versus time at different NO_2 contents. Clearly, the soot oxidation activity increases with the increasing the NO_2 concentration. Such a promoting effect is particularly evident at the lowest investigated NO_2 concentrations (e.g. in the 60–200 ppm range) while at concentrations above 200 ppm a minor increase is apparent. In particular, surface saturation effects are visible at the highest investigated NO_2 inlet concentrations, i.e. 400 and 500 ppm, where the results are nearly superimposed. The contribution of molecular oxygen to the soot oxidation has also been analyzed in this case and showed in Fig. 2D in terms of (ΔO—NO) values vs. soot conversion ζ, for the different investigated NO_2 concentrations. From Fig. 2D it clearly appears that the participation of gaseous O_2 in soot combustion is favored at high NO_2 inlet concentration, and shows a saturation effect above 400 ppm NO_2. Also during these experiments the CO_2/CO ratio has been found to be almost independent on the soot conversion and always in the range 2.5–3.5 for all the investigated NO_2 concentrations.

Finally, the influence of the NO_2 concentration on the soot oxidation was investigated at 300°C in the presence of water but without oxygen. Of note, at variance from the experiments performed in the presence of oxygen, in this case the CO_2 and CO concentration traces (data here not reported) decreased with time on stream without showing any maximum, i.e. the rate of soot oxidation decreases with the soot conversion. In line with the results of the previous experiments (Fig. 2C), it was found that also in this case the soot oxidation activity increases upon increasing the NO_2 inlet concentration from 100 to 500 ppm (Fig. 2E). Oxygen plays a relevant role in the oxidation, as can be seen by comparing the traces at the same NO_2 concentration of Fig. 2C and E. As a matter of fact, with 300 ppm of NO_2 in the feed stream and in the absence of oxygen the amount of residual soot approaches 20% (e.g. 80% conversion) after ca. 69,000 s (see Fig. 2E) while in the presence of oxygen the same conversion is attained much faster, i.e. after ca. 28,000 s (see Fig. 2C). The same beneficial effect of oxygen is evident with all the other investigated NO_2 inlet concentrations (i.e. 100 and 500 ppm). As expected, in this case the values of the (ΔO–NO) parameter as function of the soot conversion ζ are centered near zero (see Fig. 2F), because in the absence of O_2 all the oxygen provided for the soot oxidation comes from NO_2.

During these experiments the CO_2/CO ratio in the formed CO_x does not depend on the NO_2 concentration in the investigated range. However a slightly lower CO_2/CO ratio, near 2.5–3, has been measured if compared to the experiments performed in the presence of O_2. This is in line with the higher oxidation activity of the NO_2—O_2 gas mixture with respect to pure NO_2, which favors both soot combustion and CO_2 formation.

From the bulk of the data reported above, it is clear that the combustion of soot is greatly enhanced in the presence of NO_2 with respect of pure oxygen. As a matter of fact, soot oxidation is observed at 300°C in the presence of both NO_2 and O_2, but not of only oxygen. This observation is in agreement with several literature reports indicating the NO_2 as a better oxidant than O_2, which can oxidize soot at relatively low temperatures (Jelles et al., 1999; Setiabudi et al., 2002; Stanmore et al., 2001, 2008). However oxygen participates in the reaction, as pointed out by the parameter ΔO (= $2CO_2 + CO$) (see Fig. 1). Hence this indicates a cooperative effect between O_2 and NO_2 towards soot oxidation when they are both present in the feed gas. In line with mechanistic indications taken from literature (Jeguirim et al., 2005; Muckenhuber and Grothe, 2006; Setiabudi et al., 2004; Stanmore et al., 2008; Tighe et al., 2012), it can be suggested that soot oxidation is initiated at low temperatures by NO_2 via formation of oxygen complexes on the carbon surface (C(O) species), eventually resulting in the formation of CO and/or CO_2 according to reactions (4) to (6) of the following simplified mechanistic scheme:

$$C—C + NO_2 \rightarrow C—C(NO_2) \rightarrow C—C(O) + NO \quad (4)$$

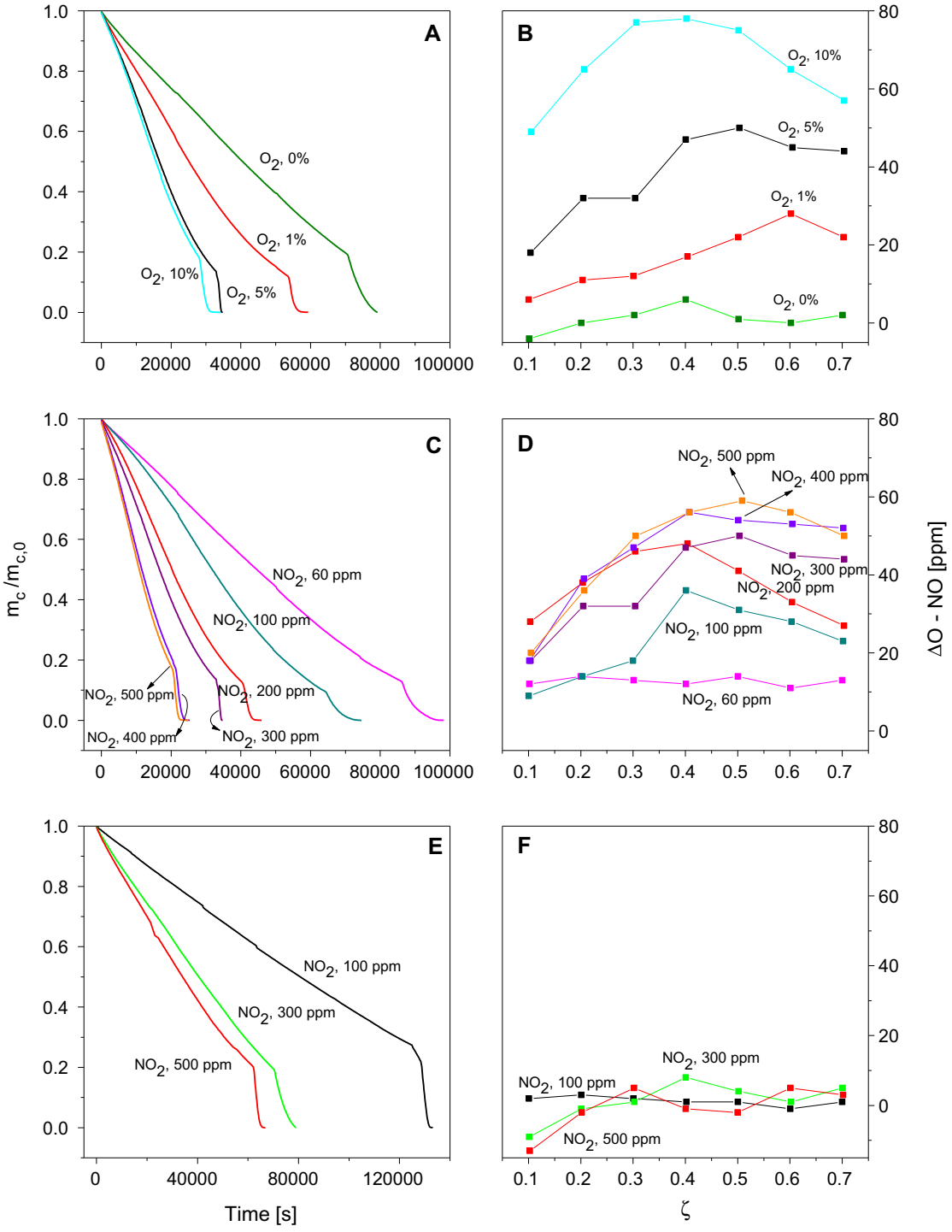

Fig. 2. Effect of oxygen concentration on Printex U oxidation in the presence of NO_2 (300 ppm): residual soot carbon mass normalized by the initial value, m_c/m_{c0} vs. time (A) and oxygen involvement in soot combustion, ΔO (= 2 CO_2 + CO) – NO vs. soot conversion ζ (B). Effect of NO_2 concentration in the presence of oxygen (5%): residual soot carbon vs. time (C) and oxygen involvement in soot combustion (D). Effect of NO_2 concentration in the absence of O_2: residual soot carbon vs. time (E) and oxygen involvement in soot combustion (F). All tests are performed at 300 °C and in presence of 2% H_2O.

$$C{-}C(O) + NO_2 \rightarrow C{-}C(NO_3) \rightarrow C(O)C(O) + NO \quad (5)$$

$$C(O)C(O) + NO_2 \rightarrow CO_2 + CO + NO \quad (6)$$

This has been pointed out by DRIFT studies (Setiabudi et al., 2004) showing the formation of different types of surface oxygen complexes (e.g. carboxylic, lactone and/or anhydride groups) as soot oxidation intermediates, upon C—NO_2 interaction.

In addition, gas phase O_2 is expected to further react with the surface oxygen complexes originated by NO_2, forming less stable complexes that decompose according to reactions (7) and (8):

$$C{-}C(O) + 1/2\ O_2 \rightarrow C(O)C(O) \quad (7)$$

$$C(O)C(O) + 1/2O_2 \rightarrow CO_2 + CO \quad (8)$$

Formation of oxygen surface complexes by NO_2 explains the participation of oxygen in the soot combustion in the presence of NO_2, even at temperatures where oxygen alone is not reactive.

Moreover, in line with this reaction scheme, it is suggested that the saturation effects observed for the O_2 concentration (see Fig. 2A and B) can be related to the fact that reactions 4 and 5, leading to the formation of the surface C oxygen complexes by NO_2, become rate limiting.

3.2. Effect of temperature

The influence of temperature on the soot combustion was investigated with the standard reactor feed (300 ppm NO_2, 5% O_2 and 2% H_2O in He) in the range 250–350 °C (i.e. 250, 263, 275, 300, 325, 337 and 350 °C). As an example, Fig. 3A and 3B show the outlet gas concentrations for the experiments carried out at the lowest and the highest investigated temperatures, i.e. 250 °C and 350 °C, respectively. In both cases the results show similar behavior with respect to the run performed at 300 °C (see Fig. 1), i.e. the evolution of CO_2, CO and NO upon NO_2 admission to the reactor at t = 0 s, due to the occurrence of soot combustion reactions (1) and (2). As expected, the soot oxidation activity increases with temperature. In fact when soot combustion is performed at 250 °C (Fig. 3A), very low levels of CO_2 and CO are observed (ca. 30 and 10 ppm, respectively, vs. 60 and 20 ppm observed at 300 °C, Fig. 1). Conversely, at the highest investigated temperature (350 °C, Fig. 3B) the production of ca. 120 and 40 ppm of CO_2 and CO, respectively, is observed. Of note, as already observed for the isothermal run performed at 300 °C, the concentration of both CO_2 and CO changes with time-on-stream, e.g. it increases during the initial stages, showing a maximum, and then decreases as soot is consumed. Notably, the maximum in the CO_x concentration is shifted to lower time-on-stream upon increasing the temperature, being near 30,000 s at 250 °C and decreasing down to 11,000 and 5000 s at 300 and 350 °C, respectively.

The effect of temperature is displayed in Fig. 4A in terms of m_C/m_{C0} (i.e. the temporal evolution of the residual soot carbon mass normalized by its initial value) versus time, for all the experiments performed in the temperature range 250–350 °C.

As expected, the rate of soot consumption increases with temperature. Temperature favors the participation of NO_2 through reactions (1) and (2), and accordingly higher NO_2 consumption can be observed during the experiment performed at 350°C (Fig. 3B) in comparison to the experiment performed at lower temperatures, e.g. 300 and 250 °C (Figs. 3A and 1, respectively). In addition, the temperature favors the participation of gaseous O_2 as shown in Fig. 4B where the values of the (ΔO—NO) parameter are plotted for the soot oxidation experiments carried out at all the investigated temperatures.

3.3. Effect of H_2O

The influence of water on the soot oxidation was investigated at 300°C by changing the inlet H_2O content from 0% to 5% in the presence of 300 ppm NO_2 and 5% O_2. The results are illustrated in Fig. 5A in terms of m_C/m_{C0} versus time. A lower oxidation activity is observed in the absence of water: in fact in this case 80% of soot conversion is reached after ca. 60,000 s while in the presence of 2%

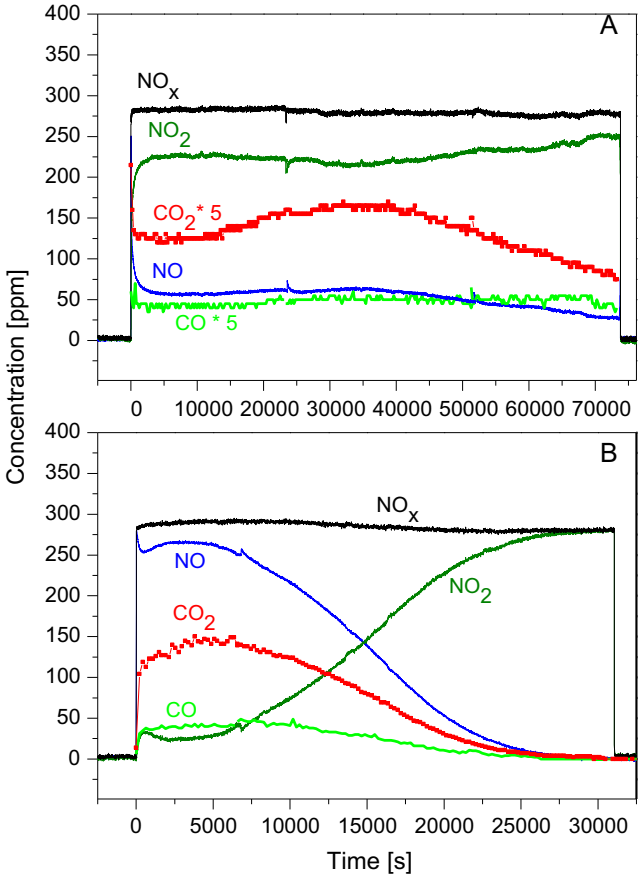

Fig. 3. Printex U oxidation at 250 °C (A) and 350 °C (B) with 300 ppm NO_2, 5% O_2 and 2% H_2O.

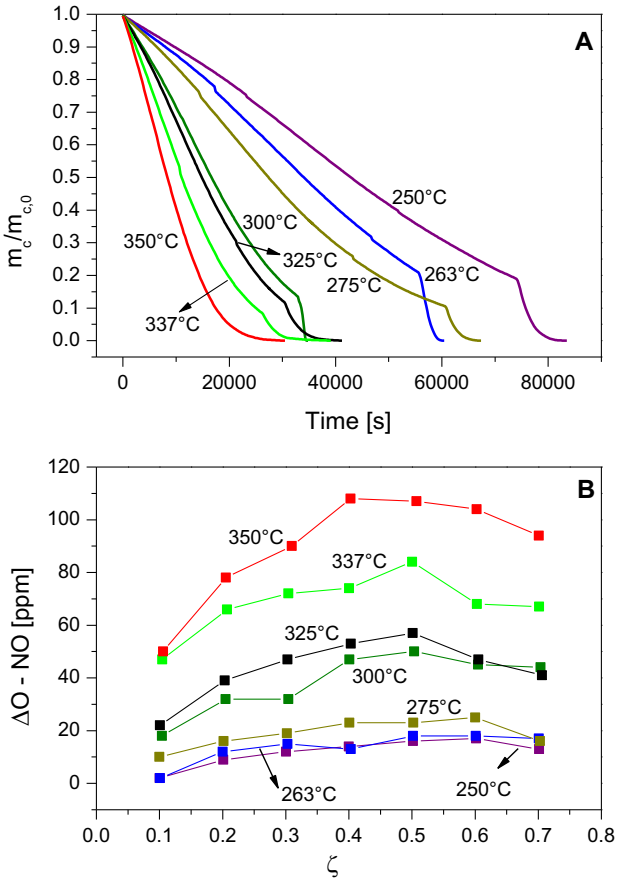

Fig. 4. Effect of temperature on Printex U oxidation: residual soot carbon mass normalized by the initial value, m_c/m_{c0} vs. time (A) and the oxygen involvement in soot combustion, ΔO (= 2 CO_2 + CO) – NO (B). All tests are performed in presence of 300 ppm NO_2, 5% O_2 and 2% H_2O in the temperature range 250–350 °C.

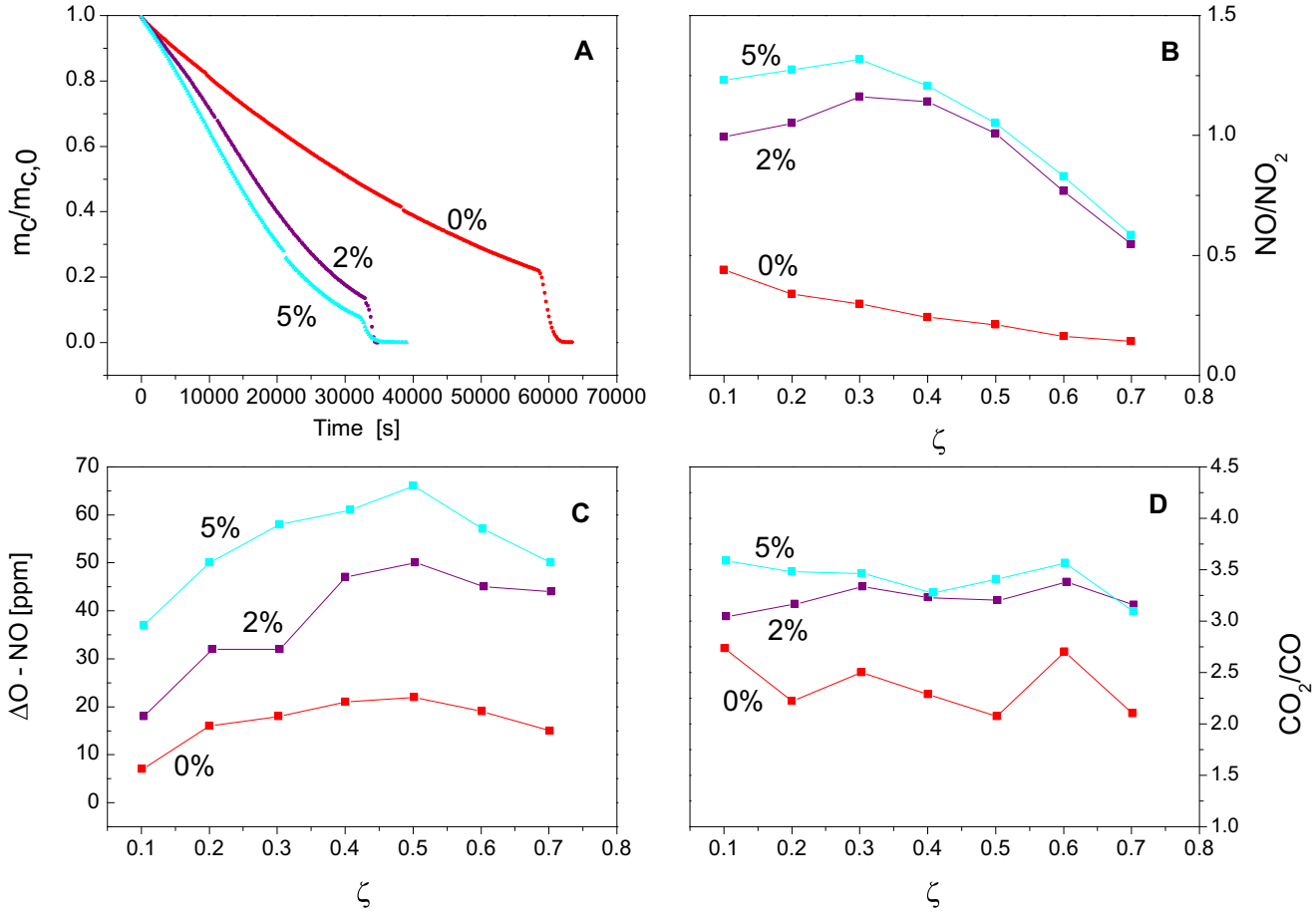

Fig. 5. Effect of water on Printex U oxidation: residual soot carbon mass normalized by the initial value, mc/m_{c0} vs. time (A); NO/NO_2 ratio vs. soot conversion ζ (B); oxygen involvement in soot combustion, ΔO(= 2 CO_2 + CO) – NO vs. soot conversion ζ (C) and CO_2/CO ratios vs. soot conversion ζ (D). All tests are performed at 300 °C and in presence of 300 ppm NO_2 and 5% O_2.

H_2O the same conversion is achieved after ca. 28,000 s. Besides the CO_2 and CO concentration traces (data not reported) didn't show any maximum but decreased with time during the test performed without water. For further increase in the inlet water concentration, up to 5%, a weak effect on soot oxidation is observed indicating the occurrence of surface saturation effects as shown in other literature reports (Messerer et al., 2006; Jung et al., 2008).

In the presence of water, the NO/NO_2 ratio (see Fig. 5B) greatly increases due to the increase of the NO_2-carbon reactivity thus leading to the higher production of NO according to reactions (1) and (2). In addition, the presence of water seems also to positive affect the participation of gaseous oxygen in soot combustion. This clearly appears from Fig. 5C showing that the (ΔO—NO) values, representative of the oxygen contribution to the soot combustion, increase upon increasing the water content.

Of note, when soot oxidation was performed in the presence of water but without O_2 (see Fig. 2F) (ΔO—NO) values always equal to zero were found, indicating that the oxygen atoms of water are not consumed for the combustion of soot by NO_2. This indicates that water seems to play a catalytic effect on both the C—NO_2 and C—O_2 reactions rather than to directly take part as a reactive species in the soot combustion. The positive effect of water on the C—NO_2 reaction has been attributed to the increased formation of oxygen complexes on carbon surface via the intermediate formation of traces of nitric and nitrous acids, which enhance the rate of the carbon oxidation by NO_2 without modifying the global mechanism reaction (Jacquot et al., 2002; Jeguirim et al., 2005, 2009b). Accordingly, such a surface activation could explain also the increasing contribution of gaseous O_2 to the carbon-NO_2 reaction.

Finally, the presence of water was found to positively affect also the CO_2 selectivity of the combustion process, which is in line with the higher soot oxidation activity observed in the presence of water and in agreement with the previous results of Neeft et al. (1997). This is shown in Fig. 5D where the CO_2/CO ratios vs. soot conversion ζ are plotted for soot oxidation experiments preformed in the absence and in the presence of water: CO_2/CO ratios in the range of 3–3.5 and 2–2.5 are observed with and without water, respectively.

3.4. Kinetic analysis

3.4.1. Reaction order of carbon

For the analysis and description of the soot oxidation data the following kinetic equation was applied:

$$(d\omega_c/dt) = -k_m(T)\omega_c^n \quad (9)$$

where ω_c is the fraction of residual soot (i.e. the residual mass of soot /initial mass of soot), k_m is the Arrhenius rate constant and n is the reaction order of soot (carbon). Both O_2 and NO_2 concentrations have been considered near-constant and homogeneous, considering the reactor to operate under differential mode. Accordingly experiments with less than 10% of NO_2 consumption were considered, whereas the oxygen consumption was small dur-

ing all the experiments. The reaction order in soot (i.e. n) was determined by applying the Eq. (9) in the linearized form (10), as it is shown in Fig. 6 for representative soot oxidation experiments:

$$ln(-d\omega_c/dT) = n\ ln(\omega_c) + ln(k_m(T)) \quad (10)$$

Fig. 6 shows that the reaction order in carbon changes with soot conversion, being negative at low conversion region and positive at high conversion region, respectively. This is in agreement with the experimental data described in the previous section, since during the run performed with the NO_2/O_2 mixture under wet conditions a maximum in the CO_2 and CO concentration traces is observed, indicating a variable dependence of the oxidation rate with soot conversion. In particular, at high conversion degree, a reaction order near 0.7 is estimated, that is close to the value of 0.67 expected from the shrinking-core model (Neeft et al., 1997) which considers soot particles as non-porous spheres with decreasing radius as the oxidation proceeds at the external particle surface.

The change of carbon reaction order with conversion and the poor accuracy of the shrinking-core model at low conversion degree have been observed also by Wang-Hansen et al. (2011) for O_2 based oxidation of Printex U. The same Authors suggested that the modification of carbon accessibility, which is likely related to changes in the surface area, can be invoked to explain the observed changes in the combustion rate during isothermal oxidation. In this respect, several studies (López-Fonseca et al., 2007; Strzelec et al., 2013; Wang-Hansen et al., 2011; Yezerets et al., 2005) showed an increase of the specific surface area of soot upon oxidation in O_2 which is remarkably greater than that predicted by the shrinking-core model. This has been explained as the development of an internal porosity during combustion rather than a conventional shrinking-core behavior *via* surface oxidation. More recently Strzelec et al. (2016) analyzed, by means of BET surface area measurements and HRTEM analyses, the burning mode of diesel particulate in NO_2, especially in comparison to oxygen. The BET results showed that, as opposed to O_2, oxidation in NO_2 alone follows the shrinking core model where only the surface carbon is being oxidized. Accordingly, the HRTEM results showed that the oxidation by O_2 proceed via opening pores leading to surface area increase in the particle (i.e. by preferentially attacking high curved lamella), while oxidation by NO_2 reacts indiscriminately upon contact with the external particulate surface. On this regard, it is worth recalling that the soot oxidation rate (indicated by the CO_2 and CO concentration traces) didn't show any maximum during the experiments performed in the presence of NO_2 only (i.e. without oxygen) which could be in agreement with a shrinking core burning mode. Interestingly, the same result was observed during the experiment performed in the absence of water. These results clearly indicate that water and oxygen promote the formation of an internal porosity upon soot oxidation in the presence of NO_2.

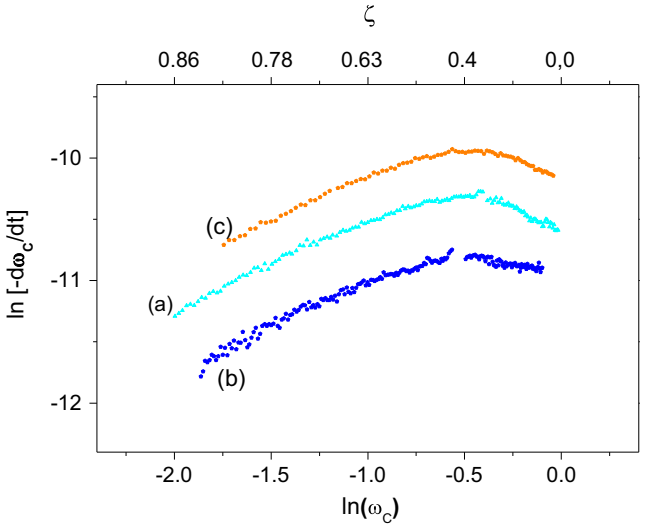

Fig. 6. Fit of reaction order in carbon for: (a) 5% O_2 2% H_2O 300 ppm NO_2 @ 300 °C; (b) 1% O_2, 2% H_2O, 300 ppm NO_2 @ 300; (c) 5% O_2 2% H_2O 500 ppm NO_2 @ 300 °C.

3.4.2. Rate coefficients and activation energy

The reaction rate constant was calculated by considering the reaction order in carbon equal to 0.7, e.g. by applying the shrinking-core model over the entire conversion interval, according to the following equation:

$$(d\omega_c/dt) = -k_m(T)\omega_c^{0.7} \quad (11)$$

Fig.7A shows the dependence of the reaction rate constant k on carbon mass conversion ζ for experiments performed with standard reactor feed (300 ppm NO_2, 5% O_2, and 2% H_2O in He) at different temperatures. At constant temperature, k_m is constant only in the high conversion region, where soot oxidation is well described by the shrinking-core model. As expected, the kinetic rate constant k_m increases with temperature, and the apparent activation energy was determined from the following equation by using an Arrhenius plot:

$$ln(k_m(T)) = ln(k_{m0}) - E_{att}/R1/T \quad (12)$$

Fig. 7B shows the Arrhenius plots for different soot conversion degrees. Of note, a decreasing activation energy with the increasing conversion has been found ranging from 44 kJ/mol at 30% conversion to 36 kJ/mol at 60% conversion, respectively. Note that the apparent value of the activation energy describes the overall oxida-

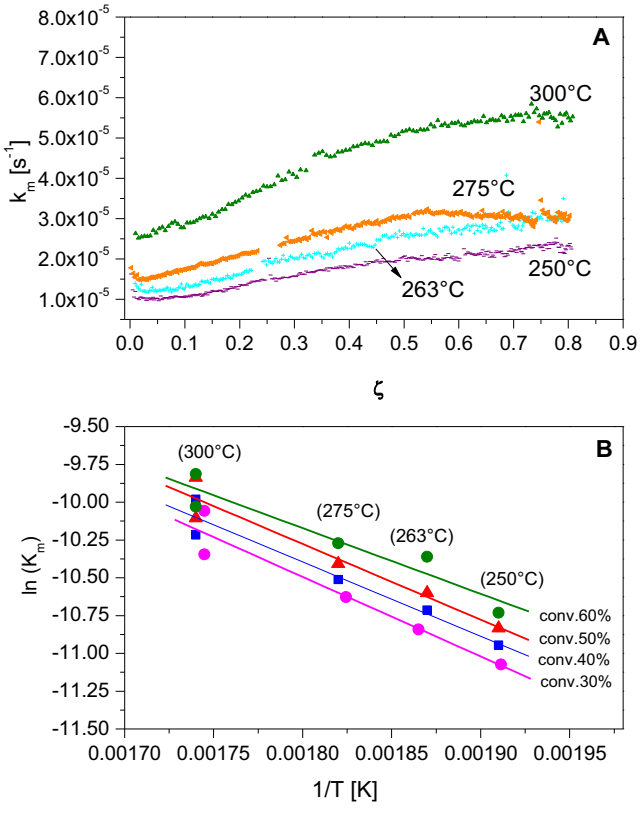

Fig. 7. Reaction rate constant vs. carbon mass conversion (A) and Arrhenius plots for different soot conversion values ζ (B) at different temperatures (with standard reactor feed: 300 ppm NO_2, 5% O_2 and 2% H_2O in He).

tion rate by NO_2 and O_2. A similar behavior has been pointed out by Wang-Hansen et al. (2011) for the O_2-based oxidation of Printex U (e.g. the activation energy was found to decrease by approximately 20 kJ/mol over all the conversion range). Along similar lines in a very recent study by Gaddam et al. (2016) the activation energy was found to vary over the course of soot oxidation depending on both the initial carbon nanostructure and structures modifications occurring during combustion. Besides, most of the studies reported single values for the overall activation energy ranging from 40 to 90 kJ/mol for soot oxidation by NO_2 and from 170 to 200 kJ/mol for soot combustion by O_2, in the temperature range 200–450 °C, depending on the different type of soot (e.g. real Diesel or model soot), as summarized by the review of Stanmore et al. (2008). Hence, the average value of the activation energy of 40 kJ/mol obtained in the present study is reasonable and in agreement with the values found by Jung et al. (2008) for the combustion of Printex U by O_2 and NO_2, under similar experimental conditions.

4. Conclusions

The non-catalytic oxidation of a synthetic soot (i.e. Printex U) has been investigated by isothermal experiments performed at different temperatures and using NO_2/O_2 mixture in a wide range of concentrations, both in the absence and in the presence of water. In the investigated reaction conditions soot oxidation is dominated by NO_2 as the main oxidant with respect to oxygen. As a matter of fact, the soot-NO_2 reaction proceeds at low temperatures, where the soot-O_2 reaction is ineffective. Besides, it has been found that soot oxidation occurs faster in the presence of both NO_2 and O_2 with respect to O_2 alone or pure NO_2, pointing out the contribution of molecular oxygen to the soot-NO_2 reaction. The oxidation of soot by NO_2 and NO_2/O_2 is enhanced by temperature. The soot oxidation rate is further increased in the presence of water possibly due to the formation of nitric and nitrous acid, whose presence seems to positively affects both soot-NO_2 reactivity and the contribution of molecular oxygen. However no direct involvement of oxygen atoms of water has been pointed out.

From the kinetic analysis, the average activation energy for soot oxidation with NO_2-O_2—H_2O was calculated near 40 kJ/mol. A non-negligible dependence of the kinetic parameters (e.g. activation energy and soot oxidation reaction order) on soot conversion was found. This outcome, together with the observed changes in oxidation rate during isothermal soot oxidation, suggests the occurrence of physicochemical changes in the carbon structure occurring during combustion.

Acknowledgements

Financial support from MIUR (Futuro in Ricerca, FIRB 2012, project SOLYST) is gratefully acknowledged.

References

Atribak, I., Bueno-López, A., García-García, A., 2010. Uncatalysed and catalysed soot combustion under NO_x + O_2: real diesel versus model soots. Combust. Flame 157, 2086–2094.

Azambre, B., Collura, S., Trichard, J.M., Weber, J.V., 2006. Nature and thermal stability of adsorbed intermediates formed during the reaction of diesel soot with nitrogen dioxide. Appl. Surf. Sci. 253, 2296–2303.

Castoldi, L., Matarrese, R., Lietti, L., Forzatti, P., 2006. Simultaneous removal of NO_x and soot on Pt–Ba/Al_2O_3 NSR catalysts. Appl. Catal. B 64, 25–34.

Cooper, B.J., Thoss, J., 1989. Role of NO in diesel particulate emission control. SAE Technical Paper 890404.

Christensen, J.M., Grunwaldt, J.-D., Jensen, A.D., 2017. Effect of NO_2 and water on the catalytic oxidation of soot. Appl. Catal. B 205, 182–188.

Fino, D., Bensaid, S., Piumetti, M., Russo, N., 2016. A review on the catalytic combustion of soot in diesel particulate filters for automotive applications: from powder catalysts to structured reactors. Appl. Catal. A 509, 75–96.

Gaddam, C.K., Vander Wal, R.L., Chen, Xu., Yezerets, A., Kamasamudram, K., 2016. Reconciliation of carbon oxidation rates and activation energies based on changing nanostructure. Carbon 98, 545–556.

Jacquot, F., Logie, V., Brilhac, J.F., Gilot, P., 2002. Kinetics of the oxidation of carbon black by NO_2 influence of the presence of water and oxygen. Carbon 40, 335–343.

Jeguirim, M., Tschamber, V., Brilhac, J.F., Ehrburger, P., 2004. Interaction mechanism of NO_2 with carbon black: effect of surface oxygen complexes. J. Anal. Appl. Pyrol. 72, 171–181.

Jeguirim, M., Tschamber, V., Brilhac, J.F., Ehrburger, P., 2005. Oxidation mechanism of carbon black by NO_2: effect of water vapour. Fuel 84, 1949–1956.

Jeguirim, M., Tschamber, V., Ehrburger, P., 2007. Catalytic effect of platinum on the kinetics of carbon oxidation by NO_2 and O_2. Appl. Catal. B 76, 235–240. Jeguirim, M., Tschamber, V., Brilhac, J.F., 2009a. Kinetics of catalyzed and non-catalyzed soot oxidation with nitrogen dioxide under regeneration particle trap conditions. J. Chem. Technol. Biotechnol. 84, 770–776.

Jeguirim, M., Tschamber, V., Brilhac, J.F., 2009b. Kinetics and mechanism of the oxidation of carbon by NO_2 in the presence of water vapor. Int. J. Chem. Kinet. 41, 236–244.

Jelles, S.J., Krul, R.R., Makkee, M., Moulijn, J.A., 1999. The influence of NO_x on the oxidation of metal activated diesel soot. Catal. Today 53, 623–630.

Johnson, T., Joshi, A., 2017. Review of vehicle engine efficiency and emissions. SAE Technical Paper 2017–01-0907.

Jung, J., Lee, J.H., Song, S., Chun, K.M., 2008. Measurement of soot oxidation with NO_2-O_2-H_2O in a flow reactor simulating diesel engine DPF. Int. J. Automotive Technol. 9, 423–428.

Leistner, K., Nicolle, A., Berthout, D., da Costa, P., 2012. Kinetic modelling of the oxidation of a wide range of carbon materials. Combust. Flame 159, 64–76.

Liu, S., Obuchi, A., Oi-Uchisawa, J., Nanba, T., Kushiyama, S., 2001. Synergistic catalysis of carbon black oxidation by Pt with MoO_3 or V_2O_5. Appl. Catal. B 30, 259–265.

Liu, J., Zhao, Z., Xu, C., Duan, A., Jiang, G., 2010. Comparative study on physicochemical properties and combustion behaviors of diesel particulates and model soot. Energy Fuels 24, 3778–3783.

López-Fonseca, R., Landa, I., Elizundia, U., Gutiérrez-Ortiz, M.A., González-Velasco, J. R., 2007. A kinetic study of the combustion of porous synthetic soot. Chem. Eng. J. 129, 41–49.

Matarrese, R., Castoldi, L., Lietti, L., Forzatti, P., 2008. Soot combustion: reactivity of alkaline and alkaline earth metal oxides in full contact with soot. Catal. Today 136, 11–17.

Matarrese, R., Castoldi, L., Artioli, N., Finocchio, E., Busca, G., Lietti, L., 2014. On the activity and stability of Pt-K/Al_2O_3LNT catalysts for diesel sootand NO_x abatement. Appl. Catal. B 144, 783–791.

Mendiara, T., Alzueta, M.U., Millera, A., Bilbao, R., 2007. Oxidation of acetylene soot: influence of oxygen concentration. Energy Fuels 21, 3208–3215.

Messerer, A., Niessner, R., Pöschl, U., 2006. Comprehensive kinetic characterization of the oxidation and gasification of model and real diesel soot by nitrogen oxides and oxygen under engine exhaust conditions: Measurement, Langmuir-Hinshelwood, and Arrhenius parameters. Carbon 44, 307–324.

Müller, J.O., Frank, B., Jentoft, R.E., Schlögl, R., Su, D.S., 2012. The oxidation of soot particulate in the presence of NO_2. Catal. Today 191, 106–111. Muckenhuber, H., Grothe, H., 2006. The heterogeneous reaction between soot and NO_2 at elevated temperature. Carbon 44, 546–559.

Nakatani, K., Hirota, S., Takeshima, S., Itoh, K., Tanaka, T., Dohmae K., 2002. Simultaneous PM and NOx reduction system for diesel engines. SAE Technical Paper 2002–01-0957.

Neeft, J.P.A., Nijhuis, T.X., Smakman, E., Makkee, M., Moulijn, J.A., 1997. Kinetics of the oxidation the diesel soot. Fuel 76, 1129–1136.

Pahalagedara, L., Sharma, H., Kuo, C.H., Dharmarathna, S., Joshi, A., Suib, S.L., Mhadeshwar, A.B., 2012. Structure and oxidation activity correlations for carbon blacks and diesel soot. Energy Fuels 26, 6757–6764.

Setiabudi, A., van Setten, B.A.A.L., Makkee, M., Moulijn, J.A., 2002. The influence of NO_x on soot oxidation rate: molten salt versus platinum. Appl. Catal. B 35, 159–166.

Setiabudi, A., Makkee, M., Moulijn, J.A., 2004. The role of NO_2 and O_2 in the accelerated combustion of soot in diesel exhaust gases. Appl. Catal. B 50, 185–194.

Sharma, H.N., Pahalagedara, L., Joshi, A., Suib, S.L., Mhadeshwar, A.B., 2012. Experimental study of carbon black and diesel engine soot oxidation kinetics using thermogravimetric analysis. Energy Fuels 26, 5613–5625.

Shirahama, N., Moon, S.H., Choi, K.H., Enjoji, T., Kawano, S., Korai, Y., Tanoura, M., Mochida, I., 2002. Mechanistic study on adsorption and reduction of NO_2 over activated carbon fibers. Carbon 40, 2605–2611.

Stanmore, B.R., Brilhac, J.F., Gilot, P., 2001. The oxidation of soot: a review of experiments, mechanisms and models. Carbon 39, 2247–2268.

Stanmore, B.R., Tschamber, V.T., Brilhac, J.F., 2008. Oxidation of carbon by NO_x, with particular reference to NO_2 and N_2O. Fuel 87, 131–146.

Strzelec, A., Toops, T.J., Daw, S.C., 2013. Oxygen reactivity of devolatilized diesel engine particulates from conventional and biodiesel fuels. Energy Fuels 27, 3944–3951.

Strzelec, A., Vander Wal, R.L., Thompson, T.N., Toops, T.J., Daw, C.S., 2016. NO_2 oxidation reactivity and burning mode of diesel particulates. Top. Catal. 59, 686–694.

Suzuki, J., Matsumoto, S., 2004. Development of catalysts for diesel particulate NO_x reduction. Top. Catal. 28, 171–176.

Sydbom, A., Blomberg, A., Parnia, S., Stenfors, N., Sandström, T., Dahlén, S.E., 2001. Health effects of diesel exhaust emissions. Eur. Respir. J. 17, 733–746.
Tighe, C.J., Twigg, M.V., Hayhurst, A.N., Dennis, J.S., 2012. The kinetics of oxidation of diesel soots by NO_2. Combust. Flame 159, 77–90.
Twigg, M.V., 2011. Catalytic control of emissions from cars. Catal. Today 163, 33–41.
van Setten, B.A.A.L., Makkee, M., Moulijn, J.A., 2001. Science and technology of catalytic diesel particulate filters. Catal. Rev. 43 (4), 489–564.
Wang-Hansen, C., Kamp, C.J., Skoglundh, M., Andersson, B., Carlsson, P.A., 2011. Experimental method for kinetic studies of gas solid reactions: oxidation of carbonaceous matter. J. Phys. Chem. C 115, 16098–16108.
Yezerets, A., Currier, N.W., Kim, D.H., Eadler, H.A., Epling, W.S., Peden, C.H.F., 2005. Differential kinetic analysis of diesel particulate matter (soot) oxidation by oxygen using a step–response technique. Appl. Catal. B 61, 120–129. Zouaoui, N., Brilhac, J.F., Mechati, F., Jeguirim, M., Djellouli, B., Gilot, P., 2010. Study of experimental and theoretical procedures when using thermogravimetric analysis to determine kinetic parameters of carbon black oxidation. J. Therm. Anal. Calorim. 102, 837–849.